Current Biology 23, 2346–2354, December 2, 2013 ©2013 Elsevier Ltd All rights reserved http://dx.doi.org/10.1016/j.cub.2013.09.056

Article

An Octopamine-Mushroom Body Circuit Modulates the Formation of Anesthesia-Resistant Memory in *Drosophila*

Chia-Lin Wu,[1,2,6] Meng-Fu Maxwell Shih,[3,6] Pei-Tseng Lee,[3] and Ann-Shyn Chiang[1,3,4,5,*]

[1]Brain Research Center, National Tsing Hua University, Hsinchu 30013, Taiwan

[2]Department of Biochemistry and Graduate Institute of Biomedical Sciences, College of Medicine, Chang Gung University, Tao-Yuan 333, Taiwan

[3]Institute of Biotechnology and Department of Life Science, National Tsing Hua University, Hsinchu 30013, Taiwan

[4]Genomics Research Center, Academia Sinica, Nankang, Taipei 115, Taiwan

[5]Kavli Institute for Brain and Mind, University of California, San Diego, La Jolla, CA 92093-0526, USA

Summary

Background: *Drosophila* olfactory aversive conditioning produces two components of intermediate-term memory: anesthesia-sensitive memory (ASM) and anesthesia-resistant memory (ARM). Recently, the anterior paired lateral (APL) neuron innervating the whole mushroom body (MB) has been shown to modulate ASM via gap-junctional communication in olfactory conditioning. Octopamine (OA), an invertebrate analog of norepinephrine, is involved in appetitive conditioning, but its role in aversive memory remains uncertain.

Results: Here, we show that chemical neurotransmission from the APL neuron, after conditioning but before testing, is necessary for aversive ARM formation. The APL neurons are tyramine, Tβh, and OA immunopositive. An adult-stage-specific RNAi knockdown of Tβh in the APL neurons or Octβ2R OA receptors in the MB α′β′ Kenyon cells (KCs) impaired ARM. Importantly, an additive ARM deficit occurred when Tβh knockdown in the APL neurons was in the *radish* mutant flies or in the wild-type flies with inhibited serotonin synthesis.

Conclusions: OA released from the APL neurons acts on α′β′ KCs via Octβ2R receptor to modulate *Drosophila* ARM formation. Additive effects suggest that two parallel ARM pathways, serotoninergic DPM-αβ KCs and octopaminergic APL-α′β′ KCs, exist in the MB.

Introduction

The fruit fly *Drosophila melanogaster* can form associative memory of an odor conditioned stimulus (CS) paired with appetitive sugar reward or aversive electrical foot shock as an unconditioned stimulus (US) [1, 2]. Mushroom bodies (MBs) integrate the olfactory CS with neuromodulatory reinforcement (US) that is thought to rely on both dopaminergic and octopaminergic signals in appetitive learning, but on only dopaminergic signaling in aversive learning [3–6]. Each MB consists of thousands of Kenyon cells (KCs) with their projections segregated into γ, α′β′, and αβ lobes (Figure S4A available online). A wealth of evidence suggests that aversive olfactory memory is initially formed through a D1-like dopamine receptor in the γ KCs, followed by communication between γ and αβ KCs to form intermediate-term memory (ITM) lasting for several hours [7, 8]. ITM is operationally divided into two forms by its susceptibility to cold-induced anesthesia: anesthesia-sensitive memory (ASM) and anesthesia-resistant memory (ARM) [9, 10]. ASM formation requires heterotypic gap-junctional communication between two MB modulatory neurons, the dorsal paired medial (DPM) neurons and the anterior paired lateral (APL) neurons [11], and normal expression of the *amnesiac* gene, which has been hypothesized to encode a putative neuropeptide in the DPM neuron [12]. ARM formation requires serotonergic neurotransmission from the DPM neurons to d5HT1A serotonin receptors in αβ KCs [13] and normal expression of the *radish* gene, which shows immunopositive signals in the αβ KCs [14].

Octopamine (OA) is synthesized from a biosynthetic pathway involving tyrosine decarboxylase (TDC) to convert tyrosine to tyramine and tyramine-β-hydroxylase (Tβh) to convert tyramine to OA [15]. Here, we show that the APL neurons release OA acting on α′β′ KCs via Octβ2R receptors to modulate ARM formation. Additive effects of OA-α′β′ KC and serotonin-αβ KC actions suggest that ARM formation has two parallel pathways in the MB.

Results

Neurotransmission from the APL Neurons Is Necessary for ARM

We first tested whether chemical neurotransmission from the two APL neurons is necessary for a 3 hr memory of aversive olfactory conditioning. Acute manipulation with dominant temperature-sensitive *shibire*^{ts1} (*shi*^{ts1}) showed that blocking neurotransmission outputs from *GH146-GAL4* containing the APL neurons (Figure 1A) during the 2 hr period after training impaired 3 hr memory retention (Figure 1B). This finding was attributed to a defect in ARM because memory impairment persisted after removing ASM with cold-induced anesthesia. In order to exclude the involvement of other neurons in *GH146-GAL4*, we identified an *APL-GAL4* line with specific expression in the two APL neurons (Figures 1C and S1) and confirmed the ARM deficit after blocking APL neurotransmission (Figure 1D).

APL Neurons Are Both GABAergic and Octopaminergic

Using an RNAi-mediated knockdown of *glutamate decarboxylase* (*Gad1*, *CG14994*), the gene encoding the synthetic enzyme for GABA, we tested whether normal levels of GABA in the APL neurons are necessary for ARM. With a full conditioning protocol to avoid the enhancement of learning by reduced γ-aminobutyric acid (GABA) levels [16], we showed that reduced GABA levels by constitutive *Gad1*^{RNAi} expression in the APL neurons (Figure S2A) did not affect 3 hr memory (Figure S2B). An adult-stage-specific *Gad1* knockdown in the APL neurons yielded the same result (Figure 2A). In order to identify the neurotransmitter involved in ARM, we performed whole-mount immunostaining using a panel of antibodies against acetylcholine transferase, GABA,

[6]These authors contributed equally to this work

*Correspondence: aschiang@life.nthu.edu.tw

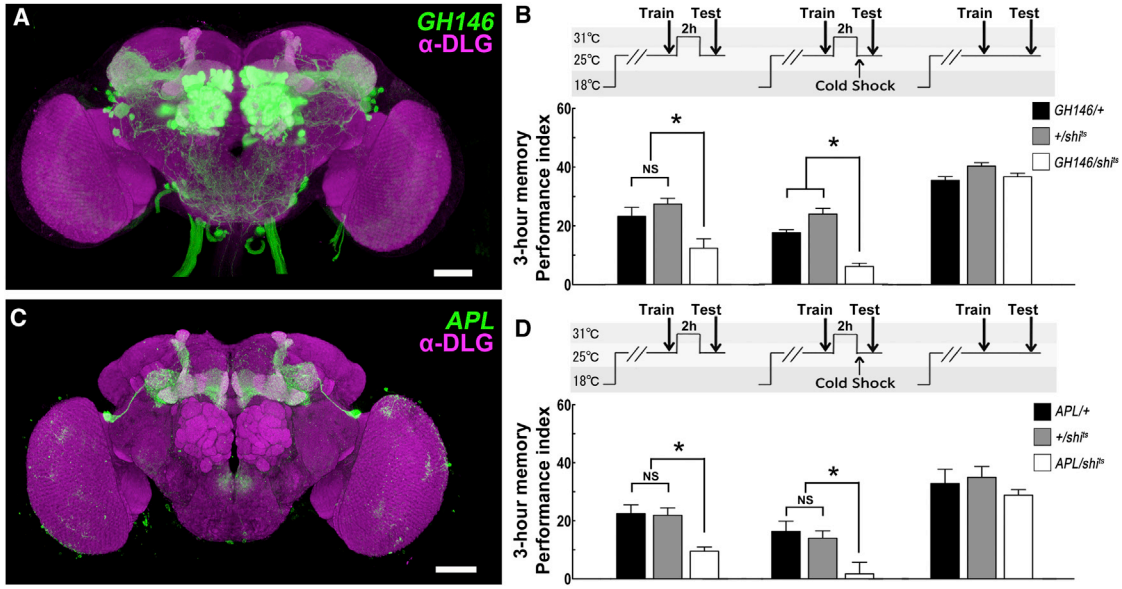

Figure 1. Blocking Neurotransmission from the APL Neurons after Training, but Before Testing, Impairs ARM

(A) The expression pattern of *GH146-GAL4* (green). The brain is immunostained with DLG antibody (magenta). The scale bar represents 50 μm. Genotype was as follows: *UAS-mCD8::GFP/+*; *GH146-GAL4/UAS-mCD8::GFP*.

(B) Effects of blocking neurotransmission from *GH146-GAL4* neurons on 3 hr memory. Neurotransmission was blocked by keeping shi^{ts1} flies at a restrictive temperature (31°C) for 2 hr immediately after training. Cold shock was applied 2 hr after training. Each value represents mean ± SEM (n = 8). *p < 0.05. Genotypes were as follows: (1) *GH146-GAL4/+*; +/+, (2) +/+; *UAS-shi*^{ts1}/+, and (3) *GH146-GAL4/+*; *UAS-shi*^{ts1}/+.

(C) The expression pattern of *APL-GAL4* (green). The brain is immunostained with DLG antibody (magenta). The scale bar represents 50 μm. Genotype was as follows: *UAS-mCD8::GFP/+*; *APL-GAL4/UAS-mCD8::GFP*.

(D) Effects of blocking neurotransmission from *APL-GAL4* neurons on 3 hr memory. Neurotransmission was blocked by keeping shi^{ts1} flies at a restrictive temperature (31°C) for 2 hr immediately after training. Cold shock was applied 2 hr after training. Each value represents mean ± SEM (n = 6–10). *p < 0.05. Genotypes were as follows: (1) +/+; *APL-GAL4/+*, (2) +/+; *UAS-shi*^{ts1}/+, and (3) +/+; *APL-GAL4/UAS-shi*^{ts1}.

See also Figure S1.

vesicular glutamate transporter, serotonin, tyrosine hydroxylase, tyramine, Tβh, and OA. Our results showed that the APL neurons are immunopositive for tyramine, Tβh, OA (Figures 2B–D), and GABA (Figure S2C). The APL neuron has a large cell body (Figure S4B) and showed weak OA-antibody immunopositive signal (Figure 2D), so we conducted additional experiments to confirm the specificity of immunostainings. First, OA-antibody immunostaining signal of the APL neuron in *Tβh*-null mutant flies was hardly detectable (Figure S2D). Quantitative comparison showed significantly lower immunostaining signals in *Tβh*-null mutant flies than in wild-type flies (Figure 2E). Second, we confirmed that the immunostaining signal to Tβh, the enzyme converting tyramine to OA, in the APL neuron was diminished in *Tβh*-null mutant flies (Figure S2E) and specifically downregulated by RNAi-mediated knockdown of *Tβh* in wild-type flies (Figure S3A). Finally, we validated the specificity of Tβh and OA immunostaining by showing that the immunostaining signal to tyramine, the substrate of Tβh enzyme, in the APL neuron remained unaffected in *Tβh*-null mutant flies (Figure S2F). Together, these data indicated that APL neurons are both GABAergic and octopaminergic.

OA in APL Neurons Is Essential for Normal ARM

Next, we showed that 3 hr memory is impaired in *Tβh*-null mutant flies with or without cold shock treatment (Figure 2F). Adult-stage-specific knockdown of *Tβh* in *GH146-GAL4* neurons impaired 3 hr memory, which was attributed to ARM deficit by additional cold shock treatment (Figure 3A). Adult-stage-specific knockdown of *Tβh* in *APL-GAL4* neurons also impaired 3 hr ARM with normal learning (Figures 3B and S3C). *Tβh* knockdown in the APL neuron also impaired 24 hr ARM after massed training (Figure S3B). These data suggest that normal OA levels in the APL neurons are essential for aversive ARM consolidation, but not for memory acquisition.

dTdc2-GAL4 expresses GAL4 under the control of a regulatory sequence of the *dTdc2* gene and hence is used routinely as a driver representing octopaminergic/tyraminergic neurons (Figure S3D; Movie S1). It covers approximately 170 octopaminergic neurons in the brain [17], but does not include the APL neurons, as indicated by GABA-antibody immunostaining (Figure S3E). Adult-stage-specific knockdown of *Tβh* in *dTdc2-GAL4* neurons did not affect 3 hr memory (Figure 3C), suggesting that most octopaminergic neurons other than the APL are not involved in ARM formation.

Axon-Dendrite Polarity of the APL Neuron

Using genetic mosaic analysis with a repressible cell marker (MARCM), we found that an APL neuron projected fibers posteriorly and innervated the whole ipsilateral MB, including the calyx and peduncle, all lobes, and contralateral β′ lobes (Figures S4A and S4B) [16]. Polarity labeling with Syt::HA, which indicated putative axonal terminals, showed an APL neuron with more presynaptic terminals in the α′β′ lobes and heel than other subregions in the MB (Figures 4A and S4C). Putative dendrites labeled with DenMark [18] were distributed more evenly among all MB subregions (Figures 4B and S4D). These

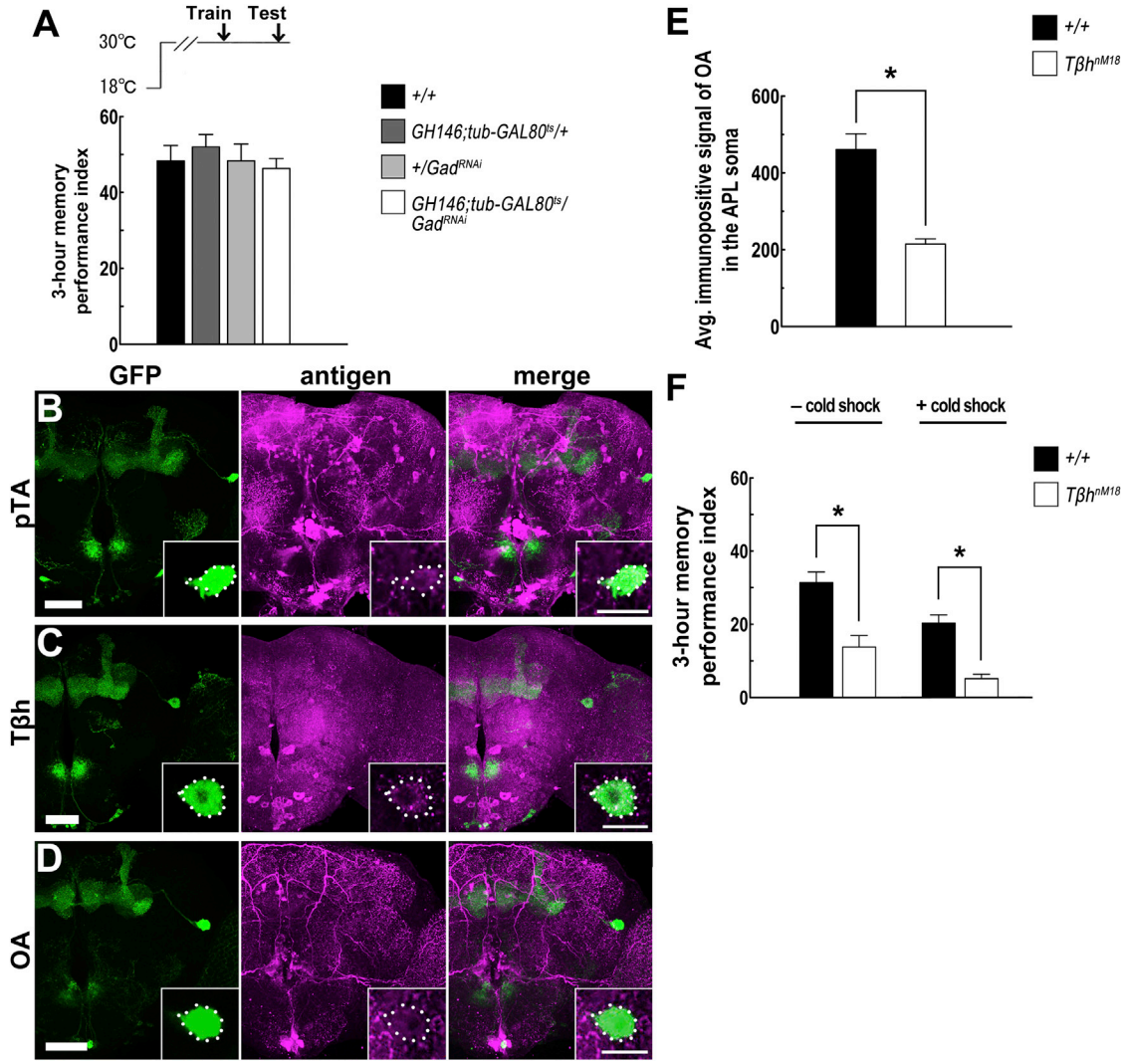

Figure 2. APL Neurons Are Both GABA- and OA-Antibody Immunopositive

(A) Effects of adult-stage-specific *Gad1* knockdown in APL neurons on 3 hr memory. Each value represents mean ± SEM (n = 8). Genotypes were as follows: (1) +/+, (2) *GH146-GAL4/+*; *tubP-GAL80^{ts}/+*, (3) +/+; +/*UAS-Gad1^{RNAi}* (v32344), and (4) *GH146-GAL4/+*; *tubP-GAL80^{ts}/UAS-Gad1^{RNAi}* (v32344).

(B) Tyramine (pTA)-antibody immunostaining (magenta) of central brain and APL soma (insets) of the *UAS-mCD8::GFP*; *APL-GAL4* fly. Scale bars represent 50 μm and 20 μm for central brain and APL soma, respectively.

(C) Tβh-antibody immunostaining (magenta) of central brain and APL soma (insets) of the *UAS-mCD8::GFP*; *APL-GAL4* fly. Scale bars represent 50 μm and 20 μm for central brain and APL soma, respectively.

(D) OA-antibody immunostaining (magenta) of central brain and APL soma (insets) of the *UAS-mCD8::GFP*; *APL-GAL4* fly. Scale bars represent 50 μm and 20 μm for central brain and APL soma, respectively.

(E) Quantitative OA-antibody immunostaining. Each value represents mean ± SEM (n = 10). *p < 0.05. Genotypes were as follows: (1) *FM7a/Y*; *UAS-mCD8::GFP/+*; *APL-GAL4/+*, and (2) *Tβh^{nM18}/Y*; *UAS-mCD8::GFP/+*; *APL-GAL4/+*.

(F) The *Tβh*-null mutants (*Tβh^{nM18}*) exhibited a 3 hr memory deficit that was further impaired by cold shock. Each value represents mean ± SEM (n = 8–10). *p < 0.05. Genotypes were as follows: (1) +/+, and (2) *Tβh^{nM18}*; +/+.

See also Figure S2.

results, together with the preferential distribution of putative synaptic active zones in the α′β′ lobes [19], predict that the α′β′ KCs are the primary downstream targets of neurotransmitters released from the APL neuron.

Octβ2R in α′β′ KCs Is Essential for ARM

Drosophila has four known OA receptors: OAMB, Octβ1R, Octβ2R, and Octβ3R [20, 21]. We used RNAi-mediated knockdown in all KCs, driven by *OK107-GAL4*, and found that ARM was impaired in flies with reduced levels of *octβ2R*, but not *oamb*, *octβ1R*, or *octβ3R* (Figure 5A). *OK107-GAL4* > *UAS-octβ2R^{RNAi}* flies exhibited normal learning (Figure S5A), suggesting that the ARM impairment was not to the result of a developmental defect. Driving *UAS-octβ2R^{RNAi}* (v104524) expression in specific subsets of MB neurons, we found that ARM formation requires normal levels of the Octβ2R receptor in the α′β′ KCs (*VT30604-GAL4*), but not in the αβ KCs (*C739-GAL4*) or γ KCs (*201Y-GAL4*) (Figure 5B). The requirement for *octβ2R* in α′β′ KCs for ARM was further confirmed by an independent RNAi line, v104050 (Figure S5C), which targets a distinct sequence of *octβ2R*. Both lines of *VT30604-GAL4* > *UAS-octβ2R^{RNAi}* (v104524 and v104050) exhibited normal

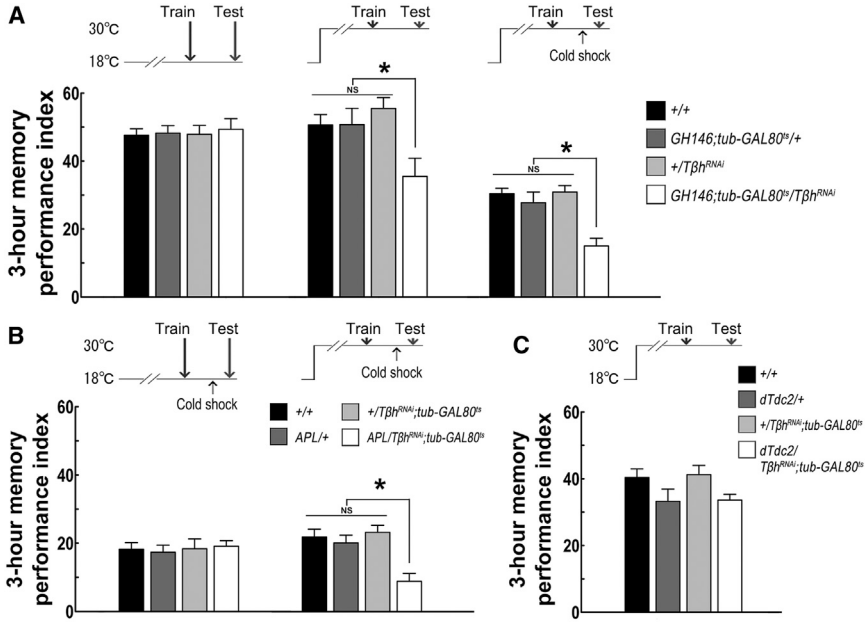

Figure 3. OA Levels in the APL Neurons Are Essential for Normal ARM

(A) Adult-stage-specific knockdown of *Tβh* in *GH146-GAL4*-containing APL neurons disrupted 3 hr ARM. Each value represents mean ± SEM (n = 8). *p < 0.05. Genotypes were as follows: (1) +/+, (2) *GH146-GAL4*/+; *tubP-GAL80^{ts}*/+, (3) +/*UAS-Tβh^{RNAi}* (v51667); +/+, and (4) *GH146-GAL4*/*UAS-Tβh^{RNAi}* (v51667); *tubP-GAL80^{ts}*/+.

(B) Adult-stage-specific knockdown of *Tβh* in *APL-GAL4*-containing APL neurons disrupted 3 hr ARM. Each value represents mean ± SEM (n = 8). *p < 0.05. Genotypes were as follows: (1) +/+, (2) +/+; *APL-GAL4*/+, (3) +/*UAS-Tβh^{RNAi}* (v51667); +/*tubP-GAL80^{ts}*, and (4) +/*UAS-Tβh^{RNAi}* (v51667); *APL-GAL4*/*tubP-GAL80^{ts}*.

(C) Adult-stage-specific knockdown of *Tβh* in *dTdc2-GAL4*-without APL neurons did not affect 3 hr ARM. Each value represents mean ± SEM (n = 8). Genotypes were as follows: (1) +/+, (2) *dTdc2-GAL4*/+, (3) +/*UAS-Tβh^{RNAi}* (v51667); *tubP-GAL80^{ts}*/+, and (4) *dTdc2-GAL4*/*UAS-Tβh^{RNAi}* (v51667); *tubP-GAL80^{ts}*/+.

See also Figure S3 and Movie S1.

learning (Figures S5B and S5C). The effectiveness of all RNAi lines used in this study was validated using quantitative PCR (qPCR) (Figure S5D). Because the qPCR results showed partial and variable knockdowns, we could not completely exclude the possibility of additional OA receptor genes being involved in this process. Western blot analysis verified a significant reduction of Octβ2R in *elav-GAL4* > *UAS-octβ2R^{RNAi}* (v104524) flies compared to control flies (Figure 5C). Because the homozygous *octβ2R* mutant flies are sterile, we confirmed the requirement of *octβ2R* for ARM again with the heterozygous *PBac{WH}octβ2R^{f05679}* mutant flies ([3, 22]; Figure 5D). Consistently, whole-mount Octβ2R immunostaining showed the preferential immunopositive signal in the α′β′ lobes and surface glia in the wild-type flies (Figures 5E and S5E) and reduced signals in the heterozygous *octβ2R* mutant flies (Figure S5F).

To rule out potential developmental effects, we next tested flies with inducible knockdown of *octβ2R* using *tubP-GAL80^{ts}* in two independent GAL4 lines, *VT30604-GAL4* and *VT57244-GAL4*, that expressed exclusively in the α′β′ KCs (Figures 6A and 6C). Our results showed that adult-stage-specific knockdown of *octβ2R* in the α′β′ KCs also impaired ARM (Figures 6B and 6D). In contrast, *octβ2R* knockdown in the APL neurons did not affect ARM (Figure 6E).

Additive Chemical and Gap-Junctional Modulations of ITM

To further evaluate the overall role of the APL neurons in ITM, we conducted a combinatorial assay involving knockdown of the ASM-required *inx7* [11] and/or ARM-required *Tβh* (Figure 7A). Compared to control flies (Figure 7A, a), 3 hr memory was impaired in flies expressing either *inx7^{RNAi}* (Figure 7A, b) or *Tβh^{RNAi}* (Figure 7A, c) in the APL neurons. Double *inx7* and *Tβh* knockdowns in the APL neurons further reduced 3 hr memory (Figure 7A, d). Cold-induced anesthesia also impaired 3 hr memory (Figure 7A, e), which was further reduced in the *Tβh* knockdown flies (Figure 7A, g), but not in the *inx7* knockdown flies (Figure 7A, f). Knockdown of *Tβh* further reduced 3 hr memory in flies already with cold-induced anesthesia and *inx7* knockdown (Figure 7A, f and h). Thus, similar to the DPM neurons [11, 13], the APL neurons modulate both ASM and ARM formations.

Octopaminergic APL and Serotoninergic DPM in ARM Formation

Next, differences in neurotransmitters and their downstream receptors prompt us to further address the relationship between octopaminergic APL and serotoninergic DPM neurons in ARM formation. ARM is impaired in the *radish* mutant (*rsh^{1}*) flies [23] or wild-type flies fed with DL-p-chlorophenylalanine (pCPA), a serotonin synthesis inhibitor [13, 24]. Lacking additive effect suggests that these two manipulations act on the same pathway in ARM formation [13]. Interestingly, we found that 3 hr ARM was further reduced in flies subjected to pCPA feeding plus *Tβh* knockdown in the APL neurons (Figure 7B). A similar additive effect was observed in the *rsh^{1}* mutant flies plus *Tβh* knockdown in the APL neurons (Figure 7C). Together, these results suggest that the octopaminergic APL neurons and the serotoninergic DPM neurons independently modulate ARM formation in different MB lobes.

Discussion

OA in Olfactory Memory

The key finding of our study is that OA from the single APL neuron innervating the entire MB is required specifically for ARM formation in aversive olfactory conditioning in *Drosophila*. This conclusion is supported by five independent lines of evidence. First, blocking neurotransmission from APL neurons after training, but before testing, impaired ARM (Figures 1B and 1D). Second, the APL neurons are tyramine, Tβh, and OA antibody immunopositive (Figures 2B–2D). Third, adult-stage-specific reduction of Tβh levels in the APL neurons, but not in *dTdc2-GAL4* neurons that do not include the APL neurons, specifically abolished ARM without affecting learning or ASM (Figures 3 and S3). Fourth, Octβ2R is expressed preferentially in the α′β′ lobes (Figure 5E), and adult-stage-specific reduction of Octβ2R expression in the α′β′ KCs impaired ARM (Figure 6). Fifth, the additive memory

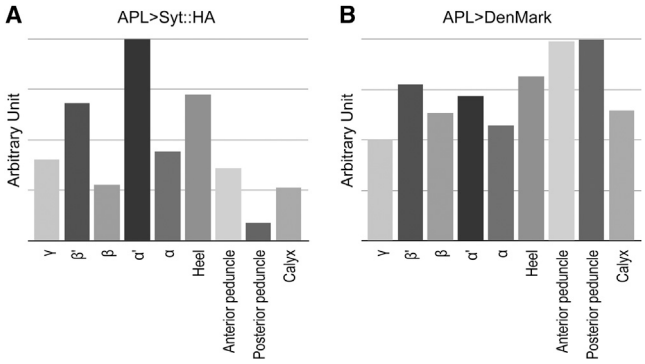

Figure 4. Quantitative Axon-Dendrite Polarity Analysis of an APL Neuron

(A) Distribution of Syt::HA-positive fibers in different MB parts.

(B) Distribution of DenMark-positive fibers in different MB parts. See Figures S4C and S4D for original images.

See also Figure S4.

impairments demonstrated in flies subjected to *Tβh* plus *inx7* knockdowns and *Tβh* knockdown plus cold shock, but not *inx7* knockdown plus cold shock, confirm that a single APL neuron modulates both ASM and ARM through gap-junctional communication and OA neurotransmission, respectively (Figure 7A). Although it has been shown that the APL neurons are also GABAergic [16], our results showed that OA is the primary neurotransmitter from the APL neurons involved in ARM formation because reduced GABA levels induced by *Gad1*^{RNAi} inhibition in the APL neurons did not affect 3 hr memory (Figures 2A, S2A, and S2B).

In *Drosophila* olfactory memories, OA and dopamine have been shown to act as appetitive and aversive US reinforcements, respectively [4]. It is important to point out that the original claim that *Tβh* plays no role in aversive learning only examined 3 min memory, not 3 hr memory or ARM [4]. It is not surprising to find that OA modulates ARM in aversive memory because dopamine has also been attributed to diverse memory roles, including a motivation switch for appetitive ITM [25] and appetitive reinforcement [3, 6, 7]. Intriguingly, dopamine negatively inhibits ITM formation [24, 26], but OA positively modulates ARM formation.

Food deprivation in *Drosophila* larvae induces behavioral plasticity and the growth of octopaminergic arbors via Octβ2R-mediated cyclic AMP (cAMP) elevation in an autocrine fashion [22]. In this study, we showed that the APL neurons release OA acting on the Octβ2R-expressing α′β′ KCs for ARM, instead of inducing autocrine regulation (Figures 5 and 6). Applying OA directly onto the adult brain results in an elevation of cAMP levels in the whole MB [27], and OA has been shown to upregulate protein kinase A (PKA) activity in the MBs [28]. Intriguingly, ARM is enhanced by a decreased PKA activity [29] and required DUNCE-sensitive cAMP signals [30]. We speculate that APL-mediated activation of Octβ2R may lead to an intricate regulation of cAMP in the α′β′ KCs for ARM formation.

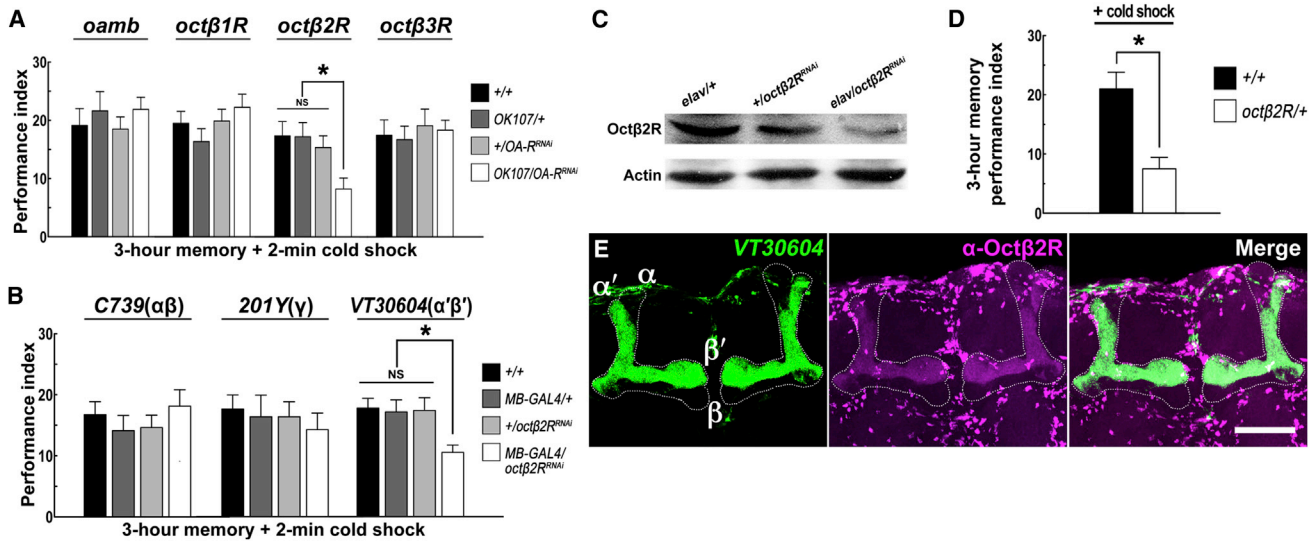

Figure 5. OA Acts on Octβ2R in α′β′ KCs for ARM Formation

(A) Effects of knockdown of OA receptors in all KCs (*OK107-GAL4*) on ARM. Three-hour memory was measured in flies subjected to a 2 min cold shock 2 hr after training. Each value represents mean ± SEM (n = 8). *p < 0.05. Genotypes were as follows: (1) +/+, (2) +/+; +/+; *OK107-GAL4*/+, (3) +/*OA-R*^{RNAi}; +/+; +/+, and (4) +/*OA-R*^{RNAi}; +/+; *OK107-GAL4*/+. *UAS-oamb*^{RNAi} (v106511), *UAS-octβ1R*^{RNAi} (v47896), *UAS-octβ2R*^{RNAi} (v104524), and *UAS-octβ3R*^{RNAi} (v101189) were used in "*OA-R*^{RNAi}" to knock down *oamb*, *octβ1R*, *octβ2R*, and *octβ3R*, respectively.

(B) Effects of *octβ2R* knockdown in subsets of MB neurons on 3 hr ARM. Each value represents mean ± SEM (n = 8). *p < 0.05. Genotypes were as follows: (1) +/+, (2) *MB-GAL4*/+, (3) +/*UAS-octβ2R*^{RNAi} (v104524), and (4) *MB-GAL4*/*UAS-octβ2R*^{RNAi} (v104524). For "*MB-GAL4*," *C739-GAL4*, *201Y-GAL4*, and *VT30604-GAL4* were used to drive *UAS-octβ2R*^{RNAi} expression in αβ, γ, and α′β′ KCs, respectively.

(C) Western blot validation of the specificity of Octβ2R antibody and the effectiveness of *UAS-Octβ2R*^{RNAi} driven by the panneuronal *elav-GAL4*. Genotypes were as follows: (1) *elav-GAL4*/+; +/+, (2) +/+; +/*UAS-octβ2R*^{RNAi} (v104524), and (3) *elav-GAL4*/+; +/*UAS-octβ2R*^{RNAi} (v104524).

(D) The heterozygous flies of the *octβ2R* mutant exhibited a 3 hr ARM deficit. Each value represents mean ± SEM (n = 8). *p < 0.05. Genotypes were as follows: (1) +/+ and (2) *PBac{WH}octβ2R*^{f05679}/+.

(E) Preferential Octβ2R expression in α′β′ lobes. *VT30604-GAL4* expression (green) and Octβ2R-antibody immunostaining (magenta) are colocalized at α′β′ lobes (merge). The MB α, α′, β, and β′ lobes are indicated by dotted lines. The scale bar represents 50 μm. Genotype was as follows: *UAS-mCD8::GFP*; *VT30604-GAL4*.

See also Figure S5.

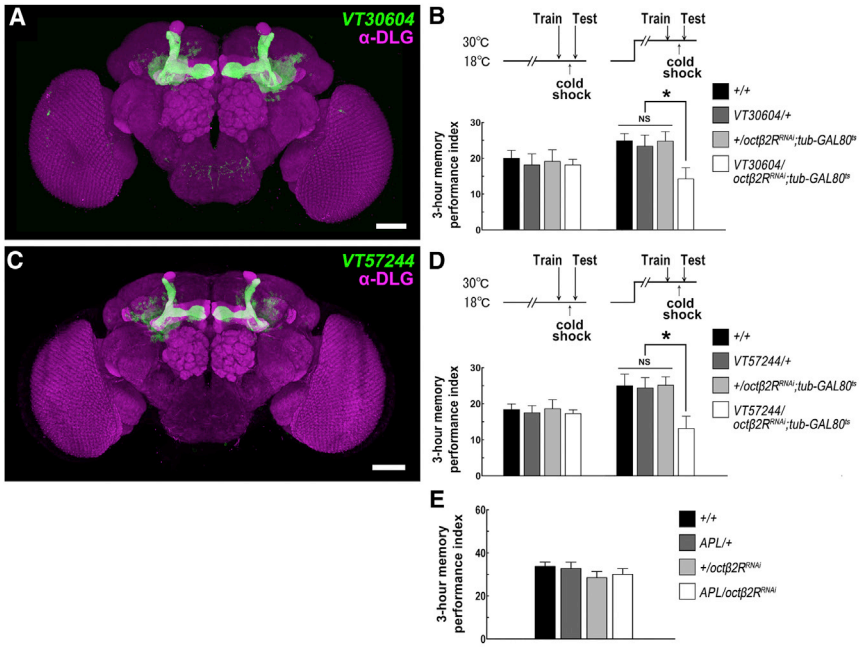

Figure 6. Effects of Adult-Stage-Specific *octβ2R* Knockdown on ARM

(A) Preferential expression of *VT30604-GAL4* in $\alpha'\beta'$ KCs (green). Genotype was as follows: *UAS-mCD8::GFP/+*; *VT30604-GAL4/UAS-mCD8::GFP*.

(B) Adult-stage-specific knockdown of *octβ2R* in *VT30604-GAL4* neurons impaired 3 hr ARM. Each value represents mean ± SEM (n = 8). *p < 0.05. Genotypes were as follows: (1) +/+, (2) +/+; *VT30604-GAL4/+*, (3) *+/UAS-octβ2R^{RNAi}* (v104524); *+/tubP-GAL80^{ts}*, and (4) *+/UAS-octβ2R^{RNAi}* (v104524); *VT30604-GAL4/tubP-GAL80^{ts}*.

(C) Preferential expression of *VT57244-GAL4* in $\alpha'\beta'$ KCs (green). Genotype was as follows: *UAS-mCD8::GFP/+*; *VT57244-GAL4/UAS-mCD8::GFP*.

(D) Adult-stage-specific knockdown of *octβ2R* in *VT57244-GAL4* neurons disrupted 3 hr ARM. Each value represents mean ± SEM (n = 8). *p < 0.05. Genotypes were as follows: (1) +/+, (2) +/+; *VT57244-GAL4/+*, (3) *+/UAS-octβ2R^{RNAi}* (v104524); *+/tubP-GAL80^{ts}*, and (4) *+/UAS-octβ2R^{RNAi}* (v104524); *VT57244-GAL4/tubP-GAL80^{ts}*.

(E) Knockdown of *octβ2R* in APL neurons did not affect 3 hr ARM. Each value represents mean ± SEM (n = 8). Genotypes were as follows: (1) +/+, (2) +/+; *APL-GAL4/+*, (3) *+/UAS-octβ2R^{RNAi}* (v104524); +/+, and (4) *+/UAS-octβ2R^{RNAi}* (v104524); *APL-GAL4/+*.

In (A) and (C), the brains are immunostained with DLG antibody (magenta). Scale bars represent 50 μm. In (B) and (D), *GAL80^{ts}* inhibition on *GAL4* expression was removed by keeping flies at 30°C for 7 days before training.

Cotransmission of GABA and OA

Although it has generally been assumed that, in a particular neuron, the same neurotransmitter is used at all synapses, exceptions continue to accumulate in both vertebrates and invertebrates. Scattered evidence suggests that corelease may be regulated at presynaptic vesicle filling and postsynaptic activation of receptors, but the physiologic significance remains poorly understood [31]. Here, we report that the APL neurons corelease GABA and OA. In the APL neurons, a reduced GABA level affects learning [16], but not ITM (Figure 2A), whereas a reduced OA level has no effect on learning (Figure S3C), but impairs ITM (Figure 3), suggesting that the two neurotransmitters are regulated in different ways in the same cell.

It has been proposed that the APL neurons might be the *Drosophila* equivalent of the honeybee GABAergic feedback neurons, receiving odor information from the MB lobes and releasing GABA inhibition to the MB calyx [16, 32, 33]. This negative feedback loop for olfactory sparse coding has been supported by electrophysiological recording of the giant GABAergic neuron in locusts [34]. However, the function of *Drosophila* APL neurons is complicated by the existence of functioning presynaptic processes in the MB lobes [16], mixed axon-dendrite distribution throughout the whole MB (Figure 4), and GABA/OA cotransmission (Figures 2 and S2).

ARM Circuit

Normal performance of ARM behavior requires serotonin from the DPM neurons acting on $\alpha\beta$ KCs via d5HT1A serotonin receptors [13] and function of RADISH [14, 23] and BRUCHPILOT [35] in the $\alpha\beta$ KCs. Surprisingly, our results show that ARM formation also requires OA from the APL neurons acting on the $\alpha'\beta'$ KCs via Octβ2R OA receptors, suggesting the existence of two distinct anatomical circuits involved in ARM formation. However, it remains uncertain whether two branches of ARM occur in parallel because combination of various molecular disruptions (i.e., *Tβh^{RNAi}* and pCPA feeding/*rsh^{1}* mutant) did not completely abolish ARM and partial disruption of one anatomical circuit will allow additive effects of another treatment even if they act on the same ARM. We favor the hypothesis of the existence of two distinct forms of ARM based on the following observations. First, neither *d5HT1A^{RNAi}* knockdown in $\alpha'\beta'$ KCs [13] nor *octβ2R^{RNAi}* knockdown in $\alpha\beta$ KCs (Figure 5) affects ARM, suggesting that the two signaling pathways act separately in different KCs and do not affect each other in the same KCs. Second, each of the three ways of molecular disruption (i.e., *Tβh^{RNAi}*, pCPA feeding, and *rsh^{1}* mutant) results in a similar degree of ARM impairment, but additive effect did not occur in *rsh^{1}* mutant flies fed with pCPA [13] and was evident when *Tβh^{RNAi}* treatment combines with either pCPA feeding or *rsh^{1}* mutant (Figures 7B and 7C). It's noteworthy that ARM is also affected by dopamine modulation because calcium oscillation within dopaminergic MB-MP1 and MB-MV1 neurons controls ARM and gates long-term memory [24], albeit a different view has been brought up [26]. The target KCs of these dopaminergic neurons on ARM remain to be addressed.

Both the APL and DPM neurons are responsive to electric shock and multiple odorants [11, 16, 36], suggesting that they likely acquire olfactory associative information during learning for subsequent ARM formation. However, the DPM neurons may receive ARM information independently because their fibers are limited within MB lobes (Figure S4E) and gap-junctional communications between the APL and DPM neurons are specifically required for the formation of ASM, but not ARM [11]. Given that all dopamine reinforcement comes in via the γ KCs [8], it is possible that the DPM neurons obtain ARM information from γ KCs. Together, these data suggest that two parallel neural pathways, serotoninergic DPM-$\alpha\beta$ KCs and octopaminergic APL-$\alpha'\beta'$ KCs, modulate 3 hr ARM formation in the MB.

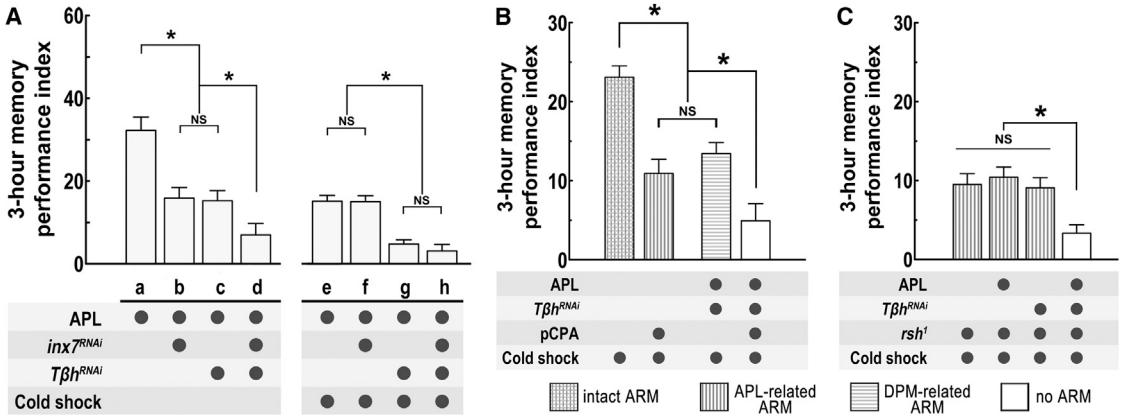

Figure 7. Additive Effects of Two ARM Pathways

(A) Additive effects of molecules in the APL neurons for ARM and ASM. Each value represents mean ± SEM (n = 8). *p < 0.05. Genotypes were as follows: (1) +/+; *APL-GAL4*/+ (a and e), (2) *UAS-inx7*^{RNAi} (v103256)/+; *APL-GAL4*/+ (b and f), (3) +/*UAS-Tβh*^{RNAi} (v51667); *APL-GAL4*/+ (c and g), and (4) *UAS-inx7*^{RNAi} (v103256)/*UAS-Tβh*^{RNAi} (v51667); *APL-GAL4*/*UAS-GAL4* (d and h).

(B) Additive effects between OA-related ARM and serotonin-related ARM. In all tests, ASM was removed by cold-induced anesthesia. Each value represents mean ± SEM (n = 12–14). *p < 0.05. Genotypes were as follows: (1 and 2) +/+; +/+ and (3 and 4) +/*UAS-Tβh*^{RNAi} (v51667); *APL-GAL4*/+.

(C) Additive effects between OA-related ARM and *radish* (*rsh*^{1})-related ARM. Each value represents mean ± SEM (n = 12). *p < 0.05. Genotypes were as follows: (1) *rsh*^{1}; +/+, (2) *rsh*^{1}; +/+; *APL-GAL4*/+, (3) *rsh*^{1}; +/*UAS-Tβh*^{RNAi} (v51667); +/+, and (4) *rsh*^{1}; +/*UAS-Tβh*^{RNAi} (v51667); *APL-GAL4*/+.

Experimental Procedures

Fly Stocks

Fly stocks were raised on standard cornmeal food at 25°C and 70% relative humidity on a 12 hr:12 hr light:dark cycle. VT lines were provided by Barry Dickson (Research Institute of Molecular Pathology, Austria). The *APL-GAL4* line was generated by recombining *VT43924-GAL4* and *UAS-GAL4* on the third chromosome. All RNAi lines were obtained from the Vienna *Drosophila* RNAi Center.

Whole-Mount Immunostaining

For octopamine and tyramine (OA/TA) staining, we used a modified version of the protocols used by Nicholas Strausfeld group [37] and Hiromu Tanimoto group [38]. After anesthetization, the fly head capsule was opened in fixative containing 0.65% glutaraldehyde in 0.1 M sodium cacodylate buffer (pH 7.0) with 1% sodium metabisulfite (SMB; Sigma-Aldrich) and prefixed for 5 min on ice. Thereafter, the fly brains were dissected and transferred into fixative containing 1.5% paraformaldehyde and 1.0% glutaraldehyde in 0.1 M sodium cacodylate buffer (pH 7.0) with 1% SMB. After twice microwave-aided fixations (2,450 MHz; 1,100 watts), 2 min on and 2 min off, the brains were treated with 0.5% sodium borohydride ($NaBH_4$; Sigma-Aldrich) in 0.05 M Tris-HCl buffer containing 0.45% SMB (Tris-HCl SMB) (pH 7.4) for 20 min to diminish autofluorescence caused by glutaraldehyde fixation. After extensive washing in Tris-HCl SMB buffer without (2 × 10 min) and with 0.5% Triton X-100 (Tris-HCl SMB TX; 2 × 10 min), the brains were incubated with 10% normal goat serum solution (NGS) diluted in Tris-HCl SMB buffer containing 2% Triton X-100 for 2 hr for OA staining or overnight for tyramine staining. All the antibodies and reagents for OA/TA staining were diluted in Tris-HCl SMB buffer containing 0.5% Triton X-100 and 10% NGS. The brains were incubated in the primary antibody, mouse-anti-OA (1:1,000; ABD-029; Jena Bioscience) or rabbit-anti-pTA (1:250 dilution; AB124; Millipore), for 2 days. After extensive washing in Tris-HCl SMB TX buffer (4 × 25 min), goat anti-rabbit or anti-mouse biotin-conjugated immunoglobulin G (IgG) (1:250 dilution; Invitrogen) was applied as secondary antibodies for 1 day. After washing (4 × 25 min), streptavidin-conjugated Alexa-635 reagent (1:500 dilution; Invitrogen) was applied to detect the immunoreactive signal.

For all other immunostainings, we used the paraformaldehyde-based procedure (Supplemental Experimental Procedures). The rat anti-Octβ2R antibody was generated by Antibody International with a high-pressure liquid chromatography (HPLC)-purified synthetic peptide, NH2-GPEPPRQRHRNRTSAARIR-COOH, selected from the Octβ2R sequence. Primary antibodies were mouse 4F3 anti-discs large antiserum (1:100 dilution; Developmental Studies Hybridoma Bank, University of Iowa), rat anti-Octβ2R antibody (1:1,000 dilution), rabbit anti-γ-aminobutyric-acid (GABA) antibody (1:250 dilution; Sigma-Aldrich), mouse 4B1 anti-choline acetyltransferase (ChAT) antibody (1:2,000 dilution; Developmental Studies Hybridoma Bank), rabbit anti-vesicular glutamate transporter (VGlut) antibody [39] (1:100 dilution), rabbit anti-serotonin antibody (1:1,000 dilution; Sigma-Aldrich), mouse anti-tyrosine hydroxylase antibody (1:50 dilution; ImmunoStar), and rabbit anti-tyramine-β-hydroxylase (Tβh) antibody [40] (1:1,000 dilution). The secondary antibodies were: 1:250 biotinylated goat anti-mouse, anti-rabbit, or anti-rat IgG (Invitrogen). Finally, brain samples were washed and incubated in 1:500 Alexa Fluor 635 streptavidin (Invitrogen) at 4°C overnight. After extensive washing, the brain samples were cleared and mounted in FocusClear (CelExplorer Labs) for confocal imaging.

Western Blotting

Brain lysate proteins were electrophoresed on 12% SDS-PAGE and then electroblotted onto polyvinylidene difluoride membranes. Immobilized proteins were probed with rat anti-Octβ2R antibody (1:20,000 dilution) or a mouse monoclonal anti-actin antibody (1:10,000 dilution; Sigma-Aldrich) as a loading control, and the membranes were incubated with horseradish peroxidase (HRP)-conjugated goat-anti-rabbit IgG secondary antibody (1:5,000 dilution). Positive signals were visualized with Qentix Western signal enhancer and SuperSignal West Pico Substrate detection (Pierce, Thermo Fisher Scientific).

Confocal Microscopy

Sample brains were imaged under a Zeiss LSM 710/510 confocal microscope with a 40 × C-Apochromat water-immersion objective lens or a 63 × LCI Plan-Neofluar objective lens.

Quantitative OA-Antibody Immunostaining

Sample brains from *FM7a/Y*; *UAS-mCD8::GFP*/+; *APL-GAL4*/+ or *Tβh*^{nM18}*/Y*; *UAS-mCD8::GFP*/+; *APL-GAL4*/+ flies were simultaneously subjected to the OA-staining protocol and imaging procedure. Images were processed with Avizo software.

Quantitative Axon-Dendrite Polarity Analysis

Images of UAS-mCD8::GFP/FRT^{g13},UAS-mCD8::GFP; UAS-syt::HA/APL-GAL4 and UAS-DenMark/FRT^{g13},UAS-mCD8::GFP; APL-GAL4/+ flies were processed with Avizo software.

Behavioral Assay

Olfactory associative learning was measured by training young adult flies (3–7 days after eclosion) in a T maze with the Pavlovian conditioning procedure.

Drug Feeding

For DL-p-chlorophenyl-alanine (pCPA), the feeding protocol has been reported in detail previously [13]. Flies, 2–3 days after eclosion, were kept in a glass bottle containing a 6 × 6 cm Chrome-Paper sheet (Sartorius) loaded with 2 ml pCPA/glucose solution overnight. pCPA (100 mg/ml; Sigma-Aldrich) was dissolved in DMSO as stock and then was diluted to 10 mg/ml in 5% glucose. The control flies were kept in a bottle with vehicle alone (2 ml 5% glucose solution without pCPA).

Statistical Analysis

All raw data were analyzed parametrically with JMP5.1 statistical software (SAS Institute). Because of the nature of their mathematical derivation, performance indices are distributed normally. Hence, the data were evaluated via one- or two-way ANOVAs, except for the two-group comparisons in the Figures 2E, 2F, and 5D, for which paired t test was applied. Subsequent pairwise planned comparisons were adjusted for experiment-wise error (α'), keeping the overall $\alpha = 0.05$. All data were presented as mean ± SEM.

Quantitative PCR

The effectiveness of each *UAS-target gene*^{RNAi} line was verified with qPCR. Flies for qPCR were generated by crossing *elav-GAL4* virgin flies to either wild-type males or the various *UAS-target gene*^{RNAi} males.

Supplemental Information

Supplemental Information includes Supplemental Experimental Procedures, five figures, and one movie and can be found with this article online at http://dx.doi.org/10.1016/j.cub.2013.09.056.

Author Contributions

C.-L.W. performed behavioral, imaging, western blot, and qPCR experiments. M.-F.M.S. performed behavioral, imaging, and qPCR experiments. P.-T.L. performed behavioral experiments. A.-S.C. analyzed the data and supervised the project.

Acknowledgments

We are grateful to Hiromu Tanimoto and Irina Sinakevitch for instructions regarding octopamine and tyramine staining. We also thank Aaron DiAntonio for the rabbit anti-dVGlut antiserum, Yi Rao for the rabbit anti-Tβh antiserum, and the Developmental Studies Hybridoma Bank for the 4F3 anti-Discs large and 4B1 anti-ChAT antibodies. We thank Vivian Budnik, Bassem Hassan, Jay Hirsh, Tzumin Lee, Liqun Luo, Yi Rao, Chun-Fang Wu, the Bloomington Drosophila Stock Center, and the Vienna Drosophila RNAi Center for fly stocks. We are especially grateful to Barry Dickson for providing unpublished VT lines. This work was supported by grants from the National Science Council and Ministry of Education in Taiwan.

Received: February 14, 2013
Revised: September 9, 2013
Accepted: September 26, 2013
Published: November 14, 2013

References

1. Tempel, B.L., Bonini, N., Dawson, D.R., and Quinn, W.G. (1983). Reward learning in normal and mutant *Drosophila*. Proc. Natl. Acad. Sci. USA *80*, 1482–1486.
2. Tully, T., and Quinn, W.G. (1985). Classical conditioning and retention in normal and mutant *Drosophila melanogaster*. J. Comp. Physiol. A Neuroethol. Sens. Neural Behav. Physiol. *157*, 263–277.
3. Burke, C.J., Huetteroth, W., Owald, D., Perisse, E., Krashes, M.J., Das, G., Gohl, D., Silies, M., Certel, S., and Waddell, S. (2012). Layered reward signalling through octopamine and dopamine in *Drosophila*. Nature *492*, 433–437.
4. Schwaerzel, M., Monastirioti, M., Scholz, H., Friggi-Grelin, F., Birman, S., and Heisenberg, M. (2003). Dopamine and octopamine differentiate between aversive and appetitive olfactory memories in *Drosophila*. J. Neurosci. *23*, 10495–10502.
5. Claridge-Chang, A., Roorda, R.D., Vrontou, E., Sjulson, L., Li, H., Hirsh, J., and Miesenböck, G. (2009). Writing memories with light-addressable reinforcement circuitry. Cell *139*, 405–415.
6. Liu, C., Plaçais, P.Y., Yamagata, N., Pfeiffer, B.D., Aso, Y., Friedrich, A.B., Siwanowicz, I., Rubin, G.M., Preat, T., and Tanimoto, H. (2012). A subset of dopamine neurons signals reward for odour memory in *Drosophila*. Nature *488*, 512–516.
7. Kim, Y.C., Lee, H.G., and Han, K.A. (2007). D1 dopamine receptor dDA1 is required in the mushroom body neurons for aversive and appetitive learning in *Drosophila*. J. Neurosci. *27*, 7640–7647.
8. Qin, H., Cressy, M., Li, W., Coravos, J.S., Izzi, S.A., and Dubnau, J. (2012). Gamma neurons mediate dopaminergic input during aversive olfactory memory formation in *Drosophila*. Curr. Biol. *22*, 608–614.
9. Margulies, C., Tully, T., and Dubnau, J. (2005). Deconstructing memory in *Drosophila*. Curr. Biol. *15*, R700–R713.
10. Quinn, W.G., and Dudai, Y. (1976). Memory phases in *Drosophila*. Nature *262*, 576–577.
11. Wu, C.L., Shih, M.F., Lai, J.S., Yang, H.T., Turner, G.C., Chen, L., and Chiang, A.S. (2011). Heterotypic gap junctions between two neurons in the *drosophila* brain are critical for memory. Curr. Biol. *21*, 848–854.
12. Waddell, S., Armstrong, J.D., Kitamoto, T., Kaiser, K., and Quinn, W.G. (2000). The *amnesiac* gene product is expressed in two neurons in the *Drosophila* brain that are critical for memory. Cell *103*, 805–813.
13. Lee, P.T., Lin, H.W., Chang, Y.H., Fu, T.F., Dubnau, J., Hirsh, J., Lee, T., and Chiang, A.S. (2011). Serotonin-mushroom body circuit modulating the formation of anesthesia-resistant memory in *Drosophila*. Proc. Natl. Acad. Sci. USA *108*, 13794–13799.
14. Folkers, E., Waddell, S., and Quinn, W.G. (2006). The *Drosophila* radish gene encodes a protein required for anesthesia-resistant memory. Proc. Natl. Acad. Sci. USA *103*, 17496–17500.
15. Monastirioti, M., Linn, C.E., Jr., and White, K. (1996). Characterization of *Drosophila* tyramine beta-hydroxylase gene and isolation of mutant flies lacking octopamine. J. Neurosci. *16*, 3900–3911.
16. Liu, X., and Davis, R.L. (2009). The GABAergic anterior paired lateral neuron suppresses and is suppressed by olfactory learning. Nat. Neurosci. *12*, 53–59.
17. Chiang, A.S., Lin, C.Y., Chuang, C.C., Chang, H.M., Hsieh, C.H., Yeh, C.W., Shih, C.T., Wu, J.J., Wang, G.T., Chen, Y.C., et al. (2011). Three-dimensional reconstruction of brain-wide wiring networks in *Drosophila* at single-cell resolution. Curr. Biol. *21*, 1–11.
18. Nicolaï, L.J., Ramaekers, A., Raemaekers, T., Drozdzecki, A., Mauss, A.S., Yan, J., Landgraf, M., Annaert, W., and Hassan, B.A. (2010). Genetically encoded dendritic marker sheds light on neuronal connectivity in *Drosophila*. Proc. Natl. Acad. Sci. USA *107*, 20553–20558.
19. Pitman, J.L., Huetteroth, W., Burke, C.J., Krashes, M.J., Lai, S.L., Lee, T., and Waddell, S. (2011). A pair of inhibitory neurons are required to sustain labile memory in the *Drosophila* mushroom body. Curr. Biol. *21*, 855–861.
20. Han, K.A., Millar, N.S., and Davis, R.L. (1998). A novel octopamine receptor with preferential expression in *Drosophila* mushroom bodies. J. Neurosci. *18*, 3650–3658.
21. Maqueira, B., Chatwin, H., and Evans, P.D. (2005). Identification and characterization of a novel family of *Drosophila* beta-adrenergic-like octopamine G-protein coupled receptors. J. Neurochem. *94*, 547–560.
22. Koon, A.C., Ashley, J., Barria, R., DasGupta, S., Brain, R., Waddell, S., Alkema, M.J., and Budnik, V. (2011). Autoregulatory and paracrine control of synaptic and behavioral plasticity by octopaminergic signaling. Nat. Neurosci. *14*, 190–199.
23. Folkers, E., Drain, P., and Quinn, W.G. (1993). Radish, a *Drosophila* mutant deficient in consolidated memory. Proc. Natl. Acad. Sci. USA *90*, 8123–8127.
24. Plaçais, P.Y., Trannoy, S., Isabel, G., Aso, Y., Siwanowicz, I., Belliart-Guérin, G., Vernier, P., Birman, S., Tanimoto, H., and Preat, T. (2012). Slow oscillations in two pairs of dopaminergic neurons gate long-term memory formation in *Drosophila*. Nat. Neurosci. *15*, 592–599.
25. Krashes, M.J., DasGupta, S., Vreede, A., White, B., Armstrong, J.D., and Waddell, S. (2009). A neural circuit mechanism integrating motivational state with memory expression in *Drosophila*. Cell *139*, 416–427.
26. Berry, J.A., Cervantes-Sandoval, I., Nicholas, E.P., and Davis, R.L. (2012). Dopamine is required for learning and forgetting in *Drosophila*. Neuron *74*, 530–542.
27. Tomchik, S.M., and Davis, R.L. (2009). Dynamics of learning-related cAMP signaling and stimulus integration in the *Drosophila* olfactory pathway. Neuron *64*, 510–521.
28. Gervasi, N., Tchénio, P., and Preat, T. (2010). PKA dynamics in a *Drosophila* learning center: coincidence detection by *rutabaga* adenylyl

cyclase and spatial regulation by *dunce* phosphodiesterase. Neuron *65*, 516–529.
29. Horiuchi, J., Yamazaki, D., Naganos, S., Aigaki, T., and Saitoe, M. (2008). Protein kinase A inhibits a consolidated form of memory in *Drosophila*. Proc. Natl. Acad. Sci. USA *105*, 20976–20981.
30. Scheunemann, L., Jost, E., Richlitzki, A., Day, J.P., Sebastian, S., Thum, A.S., Efetova, M., Davies, S.A., and Schwärzel, M. (2012). Consolidated and labile odor memory are separately encoded within the *Drosophila* brain. J. Neurosci. *32*, 17163–17171.
31. Hnasko, T.S., and Edwards, R.H. (2012). Neurotransmitter corelease: mechanism and physiological role. Annu. Rev. Physiol. *74*, 225–243.
32. Grünewald, B. (1999). Morphology of feedback neurons in the mushroom body of the honeybee, *Apis mellifera*. J. Comp. Neurol. *404*, 114–126.
33. Honegger, K.S., Campbell, R.A., and Turner, G.C. (2011). Cellular-resolution population imaging reveals robust sparse coding in the *Drosophila* mushroom body. J. Neurosci. *31*, 11772–11785.
34. Papadopoulou, M., Cassenaer, S., Nowotny, T., and Laurent, G. (2011). Normalization for sparse encoding of odors by a wide-field interneuron. Science *332*, 721–725.
35. Knapek, S., Sigrist, S., and Tanimoto, H. (2011). Bruchpilot, a synaptic active zone protein for anesthesia-resistant memory. J. Neurosci. *31*, 3453–3458.
36. Yu, D., Keene, A.C., Srivatsan, A., Waddell, S., and Davis, R.L. (2005). *Drosophila* DPM neurons form a delayed and branch-specific memory trace after olfactory classical conditioning. Cell *123*, 945–957.
37. Sinakevitch, I., and Strausfeld, N.J. (2006). Comparison of octopamine-like immunoreactivity in the brains of the fruit fly and blow fly. J. Comp. Neurol. *494*, 460–475.
38. Busch, S., Selcho, M., Ito, K., and Tanimoto, H. (2009). A map of octopaminergic neurons in the *Drosophila* brain. J. Comp. Neurol. *513*, 643–667.
39. Daniels, R.W., Collins, C.A., Gelfand, M.V., Dant, J., Brooks, E.S., Krantz, D.E., and DiAntonio, A. (2004). Increased expression of the *Drosophila* vesicular glutamate transporter leads to excess glutamate release and a compensatory decrease in quantal content. J. Neurosci. *24*, 10466–10474.
40. Zhou, C., Rao, Y., and Rao, Y. (2008). A subset of octopaminergic neurons are important for *Drosophila* aggression. Nat. Neurosci. *11*, 1059–1067.